

# Generalized synchrony of coupled stochastic processes with multiplicative noise

Haider Hasan Jafri,<sup>1</sup> R. K. Brojen Singh,<sup>2</sup> and Ramakrishna Ramaswamy<sup>2,3</sup>

<sup>1</sup>*Department of Physics, Aligarh Muslim University, Aligarh 202 002, India*

<sup>2</sup>*School of Computational and Integrative Sciences, Jawaharlal Nehru University, New Delhi 110 067, India*

<sup>3</sup>*School of Physical Sciences, Jawaharlal Nehru University, New Delhi 110 067, India*

(Received 6 August 2016; published 18 November 2016)

We study the effect of multiplicative noise in dynamical flows arising from the coupling of stochastic processes with intrinsic noise. Situations wherein such systems arise naturally are in chemical or biological oscillators that are coupled to each other in a drive-response configuration. Above a coupling threshold we find that there is a strong correlation between the drive and the response: This is a stochastic analog of the phenomenon of generalised synchronization. Since the dynamical fluctuations are large when there is intrinsic noise, it is necessary to employ measures that are sensitive to correlations between the variables of drive and the response, the permutation entropy, or the mutual information in order to detect the transition to generalized synchrony in such systems.

DOI: [10.1103/PhysRevE.94.052216](https://doi.org/10.1103/PhysRevE.94.052216)

## I. INTRODUCTION

The synchronization of rhythms is an important and extensively studied phenomenon that is ubiquitous in nature [1] and can arise in linear as well as nonlinear systems, for weak as well as strong coupling, and when the dynamics is periodic as well as when it is chaotic or otherwise complex [2–4]. This makes synchrony one of the most widely observed instances of emergent and cooperative behavior. Technological applications of synchronization are numerous, ranging from signal processing and communication protocols [5,6] to information transfer in multiprocessors [7].

Over the past decades the notion of synchrony has expanded to include the situation when distinct signals become strongly correlated without becoming identical. This is the case of the so-called generalized synchronization (GS), which was first described in the context of a skew-product (or one-way coupled) system [8]: A response system is coupled to the output of the drive, and, for sufficiently strong coupling, the output of the response is uniquely defined by the drive. Consider, for instance, the following system:

$$\dot{\mathbf{y}} = \mathbf{F}_y(\mathbf{P}_y, \mathbf{y}), \quad (1)$$

$$\dot{\mathbf{x}} = \mathbf{F}_x(\mathbf{P}_x, \mathbf{x}) + \varepsilon(\mathbf{y} - \mathbf{x}), \quad (2)$$

where the subscripts  $\mathbf{y}$  and  $\mathbf{x}$  denote the drive and the response respectively, the dynamical variables of either system are denoted by  $\mathbf{y}(t) \in \mathbb{R}^n$  and  $\mathbf{x}(t) \in \mathbb{R}^m$ ,  $\mathbf{F}_y$  and  $\mathbf{F}_x$  specify the respective  $n$ - and  $m$ -dimensional flows, and  $\mathbf{P}_{y,x}$  are the sets of parameters in the two systems. The coupling considered above is linear (diffusive), but the discussion below applies to other forms of coupling as well. GS is said to occur in the system when there is a unique functional relationship,

$$\mathbf{x} = \Phi[\mathbf{y}], \quad (3)$$

between the drive and response variables. Depending on whether  $\Phi$  is differentiable, the generalized synchronization is termed as strong or weak [9,10], and numerous studies have examined the nature and characteristics of GS in a variety of systems, including those with nonlinear coupling.

In a number of situations of practical importance, however, the microscopic dynamics is governed by a set of coupled

stochastic processes [11–14], and it is therefore of interest to examine how these ideas of synchrony can be extended to dynamical systems in which fluctuations cannot be suppressed. The present work addresses this issue in the context of coupled microscopic chemical reactions, wherein the dynamics is subject to both intrinsic and extrinsic noise and the variables therefore can undergo large fluctuations. Such a situation is common, for instance, in biological reactions at the cellular and subcellular levels. The methods of analysis that are applicable to deterministic dynamical systems [1] cannot be easily adapted in a straightforward manner to stochastic systems.

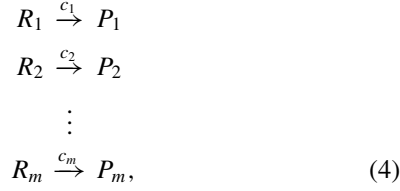
In the present work, we consider two sets of coupled chemical reactions that interact with each other. Our interest is in the manner in which the two subsystems become correlated, in a manner that is analogous to synchrony. We also approximate the master equation that describes this system by the Langevin equation [15] and study the dynamics of this system in which the noise that appears is multiplicative. One consequence is that the noise cannot be “switched off” except in the thermodynamic limit, and thus we seek measures that can assess the degree of synchrony accurately in systems that are dominated by noise.

The basic framework of our study is outlined in Sec. II, and application is made to model coupled stochastic processes. The examples we consider are chosen to correspond to well-known dynamical systems such as the Brusselator and the Lorenz system, primarily so the dynamics is well understood in the thermodynamic limit. We calculate correlations and information-theoretic measures to study the transition. The transition to generalized synchrony in case of chemical oscillators is described in Sec. III. We apply the above-discussed order parameters to these coupled systems in order to detect the transition in finite systems. We conclude with a discussion and summary in Sec. IV.

## II. STOCHASTIC DRIVE-RESPONSE SYSTEMS WITH MULTIPLICATIVE NOISE

The effect of external additive noise has been studied in detail in the context of generalized synchrony [16,17]. Our interest here is on the nature of intrinsic noise, such as might arise in systems far from the thermodynamic limit. There has

been a resurgence of interest in such “small” systems in view of the fact that the biological cell is small while being amenable to detailed study. In such systems, the various processes can be depicted as a series of  $m$  coupled chemical reactions,



where  $R_i$ ,  $P_i$ , and  $c_i$  represent, respectively, the reactant and product species and rates of the  $i$ th reaction. Depending on the nature of the different reactions and the species involved, one typically arrives at a set of coupled differential equations,

$$\dot{\mathbf{x}} = f_{\mathbf{x}}(\mathbf{x}) + \frac{g_{\mathbf{x}}(\mathbf{x})}{\sqrt{V}} \xi_{\mathbf{x}}(t) + \dots, \quad (5)$$

where the elements of the vector  $\mathbf{x}$  are the concentrations of the various species involved in the above reactions [Eq. (4)]. The functional form of the deterministic part,  $f_{\mathbf{x}}$ , as well as that of  $g_{\mathbf{x}}$  which comes from the noise part, depends on the specifics of the reaction scheme. It should be noted that one is essentially dealing with a set of coupled stochastic processes, and in the limit of the volume  $V \rightarrow \infty$ , one has the law of mass action [18], obtaining a set of coupled differential equations from a set of coupled chemical reactions [19].

Our interest in the present work focuses on the coupling between two distinct systems of coupled stochastic processes. While an explicit example will be given below, it should be noted that this is a not uncommon occurrence within the cell, when two or more regulatory pathways overlap and/or interfere [20]. This can result in the resulting differential equations being coupled, leading to unexpected correlations in the different variables, and, indeed, a form of synchrony [1].

### A. The Lorenz-Brusselator system

As an example of the scenario, we consider the so-called Brusselator model that can be derived from the set of chemical reactions described in Eq. (A1) (Appendix) [21]. The corresponding chemical Langevin equation (CLE) can be written as follows [15]

$$\begin{aligned} \dot{x}_1 &= f_1(x_1, x_2) + \frac{g_1(x_1)}{\sqrt{V}} \xi_1(t) + \frac{g_2(x_1, x_2)}{\sqrt{V}} \xi_2(t) \\ \dot{x}_2 &= f_2(x_1, x_2) + \frac{g_2(x_1, x_2)}{\sqrt{V}} \xi_2(t), \end{aligned} \quad (6)$$

where the  $\xi_i$  terms represent  $\delta$ -correlated white noise,  $\langle \xi_i(t) \rangle = 0$  with  $\langle \xi_i(t) \xi_j(t') \rangle = \delta(t - t') \delta_{ij}$ ,  $i, j = 1, 2$ . The quantities  $f_i(\mathbf{x})$ , and  $g_i(\mathbf{x})$ ,  $i = 1, 2$  are defined as

$$\begin{aligned} f_1(\mathbf{x}) &= c_1 - c_2 x_1 + c_3 x_1 (x_1 - 1) x_2 / 2 - c_4 x_1 \\ f_2(\mathbf{x}) &= c_2 x_1 - c_3 x_1 (x_1 - 1) x_2 / 2 \\ g_1(\mathbf{x}) &= \sqrt{[c_1 + c_4 x_1]} \\ g_2(\mathbf{x}) &= \sqrt{[c_2 + c_3 (x_1 - 1) x_2 / 2] x_1}. \end{aligned} \quad (7)$$

A similar set of equations for the chemical reactions can be written, and these lead to the Langevin-Lorenz system [22]

[Appendix; see Eq. (A2)],

$$\begin{aligned} \dot{x}'_1 &= -\sigma x'_1 + \sigma x'_2 + h_1(\mathbf{x}') + \varepsilon(x_1 - x'_1) \\ \dot{x}'_2 &= -x'_1 x'_3 + r x'_1 - x'_2 + h_2(\mathbf{x}') \\ \dot{x}'_3 &= x'_1 x'_2 - b x'_3 + h_3(\mathbf{x}') \end{aligned} \quad (8)$$

with the additional terms involving noise being [15]

$$\begin{aligned} h_1(\mathbf{x}') &= \frac{1}{\sqrt{V}} \{ -\sqrt{|\sigma x'_1|} \eta_1 + \sqrt{|\sigma x'_2|} \eta_2 \} \\ h_2(\mathbf{x}') &= \frac{1}{\sqrt{V}} \{ -\sqrt{|x'_1 x'_3|} \eta_3 + \sqrt{|r x'_1|} \eta_4 - \sqrt{|x'_2|} \eta_5 \} \\ h_3(\mathbf{x}') &= \frac{1}{\sqrt{V}} \{ \sqrt{|x'_1 x'_2|} \eta_6 - \sqrt{|b x'_3|} \eta_7 \} \end{aligned} \quad (9)$$

as can be derived in a straightforward manner. The diffusive coupling term in Eq. (8) represents the diffusion of the species (represented by  $x_1$ ) from one system to the other. The noises  $\eta_i$  and  $\xi_j$  are, of course, independent, and, further,  $\langle \eta_i(t) \rangle = 0$  with  $\langle \eta_i(t) \eta_j(t') \rangle = \delta(t - t') \delta_{ij}$ .

In order to assess the effect of the stochastic drive it is customary to compare the response dynamics with that of another copy [23]. Thus the same (Brusselator) drive can be coupled to a second response system that is termed the auxiliary unit. When the stochastic Brusselator drive couples to the Lorenz response and the auxiliary unit which is another replica of the response, one obtains a set of coupled stochastic equations, namely Eqs. (6) and (8), together with

$$\begin{aligned} \dot{x}''_1 &= -\sigma x''_1 + \sigma x''_2 + h_1(\mathbf{x}'') + \varepsilon(x_1 - x''_1) \\ \dot{x}''_2 &= -x''_1 x''_3 + r x''_1 - x''_2 + h_2(\mathbf{x}'') \\ \dot{x}''_3 &= x''_1 x''_2 - b x''_3 + h_3(\mathbf{x}'') \\ h_1(\mathbf{x}'') &= \frac{1}{\sqrt{V}} \{ -\sqrt{|\sigma x''_1|} \eta_8 + \sqrt{|\sigma x''_2|} \eta_9 \} \\ h_2(\mathbf{x}'') &= \frac{1}{\sqrt{V}} \{ -\sqrt{|x''_1 x''_3|} \eta_{10} + \sqrt{|r x''_1|} \eta_{11} - \sqrt{|x''_2|} \eta_{12} \} \\ h_3(\mathbf{x}'') &= \frac{1}{\sqrt{V}} \{ \sqrt{|x''_1 x''_2|} \eta_{13} - \sqrt{|b x''_3|} \eta_{14} \}. \end{aligned} \quad (10)$$

Note that there are several *independent, multiplicative* noise terms, and this is the main distinction between the present coupled stochastic system and deterministic systems with additive noise [16,17,24,25].

Simulations of the system with noise are carried out in the usual manner, integrating the equations of motion using a modified Euler’s method [26] or a similarly modified fourth-order Runge-Kutta scheme. Since the coupling is between two very dissimilar systems as evidenced by the reaction schemes [Eqs. (A1) and (A2)] or the derived differential equations [Eqs. (9) and (10)], it is useful to judge the extent to which the variables in the response system are uniquely determined by the drive.

Shown in Fig. 1 are the attractors generated by the drive-response system, projected onto the  $x_1$ - $x'_1$  and  $x'_1$ - $x''_1$  planes, where Fig. 1(a) and Fig. 1(b) are the projections for  $\varepsilon = 0$ , implying that there is no correlation between the drive-response and auxiliary units. If one increases the coupling, Fig. 1(c) and Fig. 1(d) for  $\varepsilon = 0.5$ , the two units

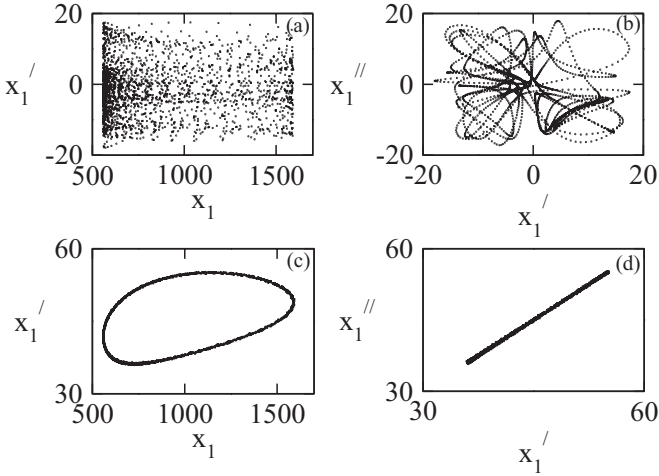


FIG. 1. Phase-space plots for Eqs. (6), (8), and (10) as a function of the coupling. Attractor in the  $x_1$ - $x_1'$  plane for the drive response system for the parameter values  $c_1 = 2.25 \times 10^4$ ,  $c_2 = 50$ ,  $c_3 = 5 \times 10^{-5}$ ,  $c_4 = 25$ ,  $V = 0.1$ ,  $\sigma = 10$ ,  $b = 8/3$ ,  $r = 28$  at (a)  $\varepsilon = 0$  and (c)  $\varepsilon = 0.5$ . Similar plots in the  $x_1'$ - $x_1''$  plane for the response and auxiliary at (b)  $\varepsilon = 0$  and (d)  $\varepsilon = 0.5$ .

are clearly synchronized. Since the response and the auxiliary unit are in complete synchrony [see Fig. 1(d)], the systems in the drive response configuration are in weak generalized synchrony [10].

The synchrony of the drive response system with increase in the coupling values can be seen in Fig. 2 as well. At  $\varepsilon = 0$  and  $\varepsilon = 0.05$  [Figs. 2(a) and 2(b)], the time series of the drive and response are uncorrelated. As the coupling increases the time series of the drive and response as well as the response and auxiliary unit begins to synchronize [Fig. 2(c)] and at large coupling  $\varepsilon = 0.5$ , the auxiliary units are strongly correlated indicating the state of GS [Fig. 2(d)].

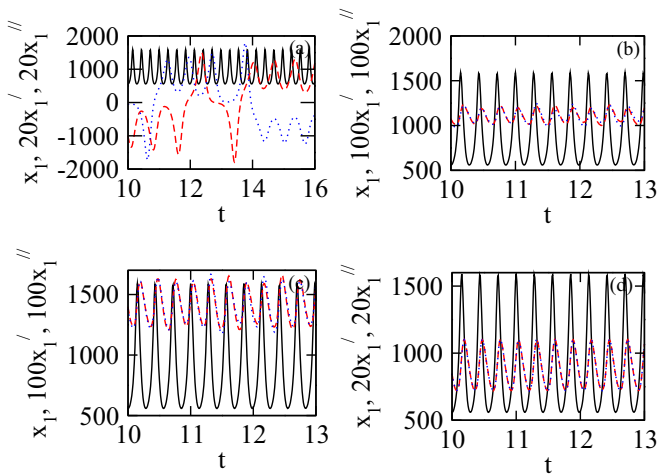


FIG. 2. Time series of the drive (solid black line), response (dotted blue line), and the auxiliary unit (dashed red line) Eqs. (6), (8), and (10) for the parameter values  $c_1 = 2.25 \times 10^4$ ,  $c_2 = 50$ ,  $c_3 = 5 \times 10^{-5}$ ,  $c_4 = 25$ ,  $V = 0.1$ ,  $\sigma = 10$ ,  $b = 8/3$ ,  $r = 28$  at (a)  $\varepsilon = 0$ , (b)  $\varepsilon = 0.05$ , (c)  $\varepsilon = 0.1$ , and (d)  $\varepsilon = 0.5$ .

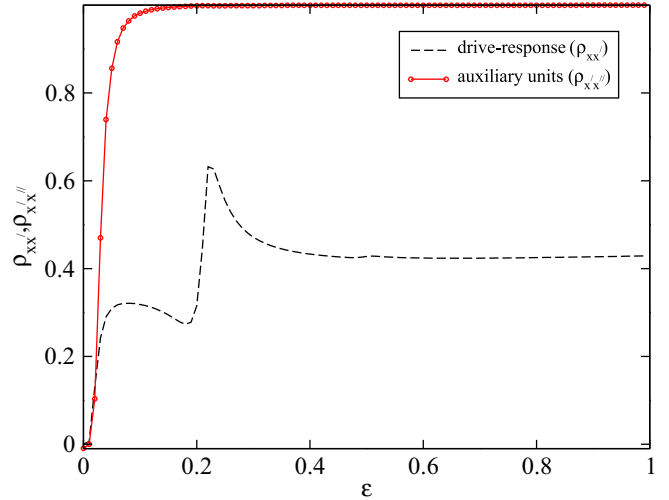


FIG. 3. Correlation for the oscillatory dynamics Eqs. (6), (8), and (10) for the parameter values  $c_1 = 2.25 \times 10^4$ ,  $c_2 = 50$ ,  $c_3 = 5 \times 10^{-5}$ ,  $c_4 = 25$ ,  $V = 0.1$ ,  $\sigma = 10$ ,  $b = 8/3$ ,  $r = 28$  between drive and response (dashed line) and between the response and the auxiliary unit (red circle).

It is preferable, however, to examine the degree of correlation between the response and its copy, the auxiliary response, through the quantity

$$\rho_{x_i x_i'} = \lim_{t \rightarrow \infty} \frac{[\langle x_i(t)x_i'(t) \rangle - \langle x_i(t) \rangle \langle x_i'(t) \rangle]}{\sigma_{x_i} \sigma_{x_i'}}, \quad (11)$$

where the  $\sigma$ 's are the standard deviations for the signals  $x_i(t)$  and  $x_i'(t)$ , respectively, and provide a good measure of the correlatedness of two variables  $x_i$  and  $x_i'$ . If  $\rho_{x_i x_i'}$  is close to 1, then the two systems can be considered to be strongly correlated while uncorrelated variables will have  $\rho_{x_i x_i'}$  significantly below 1. This measure is thus a proxy for the correlations between the drive and the response.

The variation of correlation with coupling is shown in Fig. 3. In this system, there is phase synchronization [1] between the drive and response prior to GS, and this shows up as a kink in the curve at  $\varepsilon = 0.2$ . Since the correlation between the response and the auxiliary unit is high, this feature is not visible in the corresponding curve in Fig. 3 (see, however, Fig. 4 below).

### B. Information-theoretic measures

Measures based on information theory such as the mutual information (MI) are sensitive to details of the dynamics that do not manifest themselves in simpler entities such as the correlation function [27,28]. MI measures the general dependence of two variables, and therefore it provides a more robust measure to study stochastic time series than the cross-correlation function, which only measures linear dependence.

Consider a set of  $N$  bivariate measurements  $u_i = (x_i, y_i)$  that are assumed to be independent and identically distributed realizations of random variable  $Z = (X, Y)$  with density  $\mu(x, y)$ . The marginal densities of  $X$  and  $Y$  are, respectively,

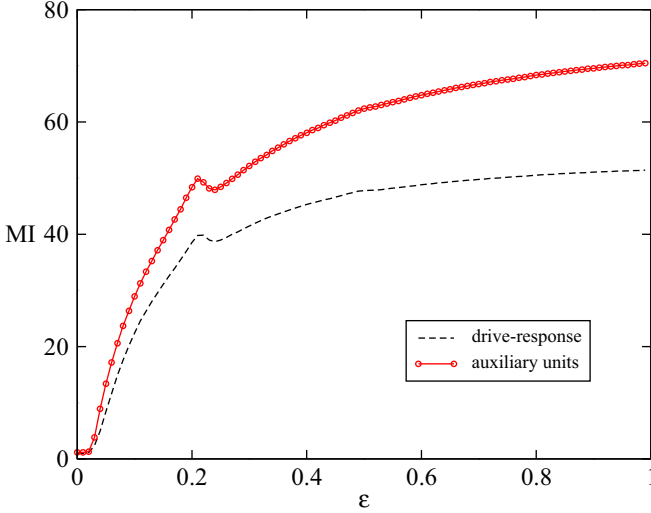


FIG. 4. Mutual information for the system given by Eqs. (6), (8), and (10) for the parameter values  $c_1 = 2.25 \times 10^4$ ,  $c_2 = 50$ ,  $c_3 = 5 \times 10^{-5}$ ,  $c_4 = 25$ ,  $V = 0.1$ ,  $\sigma = 10$ ,  $b = 8/3$ ,  $r = 28$  between drive and response (dashed line) and between the response and the auxiliary unit (red circle).

$\mu_x(x) = \int dy \mu(x, y)$  and  $\mu_y(y) = \int dx \mu(x, y)$ , and the MI is defined by

$$I(X, Y) = \int dx \int dy \mu(x, y) \ln \frac{\mu(x, y)}{\mu_x(x) \mu_y(y)}. \quad (12)$$

A computationally efficient method to evaluate the MI is to cover the phase space in bins of finite size. This can be approximated by the relation

$$I(X, Y) = \sum_{i, j} p(i, j) \log \frac{p(i, j)}{p_x(i) p_y(j)}, \quad (13)$$

where  $p_x(i) = \int_i dx \mu_x(x)$ ,  $p_y(j) = \int_j dy \mu_y(y)$ , and  $p(i, j) = \int_i dx \int_j dy \mu(x, y)$ . (Note that  $\int_i$  indicates that the integral is taken over bin  $i$ .) Numerically, if  $n_x(i)$  [ $n_y(j)$ ] is the number of points falling in  $i$ th bin of  $X$  [ $j$ th bin of  $Y$ ] and  $n(i, j)$  is the number of points falling in their intersection, then we approximate  $p_x(i) \approx n_x(i)/N$ ,  $p_y(j) \approx n_y(j)/N$ , and  $p(i, j) \approx n(i, j)/N$ , where  $N$  denotes the total number of points in a bin.

As shown in Fig. 4, the MI increases with the increase in coupling. At lower coupling values the MI between the drive-response and response-auxiliary unit is low, which increases and finally becomes constant as one increases the coupling between the two systems. The higher values of MI at larger coupling values clearly capture the onset of generalized synchrony in the system.

If the noise is additive and of low intensity, then Lyapunov exponents can also be computed in the usual manner as a function of the coupling for the drive-response system [25]. However, this is not possible here and we therefore discuss the use of the permutation entropy (PE), a complexity measure that can be easily calculated for any time series [29]. In model systems it has been observed that the PE behaves very similarly to the Lyapunov exponent over a wide range of parameter

values, which suggests that the PE can be used as a proxy for the Lyapunov exponent.

We briefly recall the methodology outlined in Ref. [29]. Given a stationary time series  $\{x_t\}$ , which attains a finite number  $M$  of values, the classical source Shannon entropy  $h$  lies in the interval  $[0, \log M]$ . When  $\{x_t\}$  takes arbitrary values, it is simpler to coarse grain the series and replace the discrete values by a symbolic sequence  $\{s_t\}$  with a finite number of symbols. The source entropy for the symbolic sequence  $s_t$  is computed in the usual manner [29]. For a given series one studies all  $n!$  permutations  $\pi$  for which the relative frequency is given by

$$p(\pi) = \frac{t | t \leq T - n, (x_{t+1}, \dots, x_{t+n}) \text{ has type } \pi}{T - n + 1}. \quad (14)$$

The permutation entropy of order  $n \geq 2$  is defined as

$$H(n) = - \sum p(\pi) \log p(\pi), \quad (15)$$

where the sum runs over all the  $n!$  permutations  $\pi$  of order  $n$ . The permutation entropy per symbol of order  $n$  is

$$h_n = H(n)/(n - 1) \quad (16)$$

since the time series  $h_n$  typically changes with time. For two nearly identical time series or for two time series in synchrony, although one cannot expect them to have identical PE, the manner in which these change (the trend) should be identical since the two time series are in synchrony. One can transform the trend into a symbolic string to estimate the correlation and thereby construct an order parameter  $\gamma$  [30].

For a time series of length  $N$ , we divide these into equal number of smaller intervals, say,  $n_1, n_2, \dots$  such that  $\sum_i n_i = N$ . The value of  $n_i$  as well as  $i$  should be large enough to avoid statistical errors. Thus we have a set of permutation entropies  $\{h_i\}$  corresponding to each interval of the time series. Consider a variable  $c_i$  such that  $c_i = 1$  if  $h_i > h_{i-1}$  and  $c_i = -1$  otherwise for one time series. A similar sequence can be obtained for the other time series,  $c'_i$ . The order parameter  $\gamma$  [30] is then defined as

$$\gamma = \langle c_i c'_i \rangle, \quad (17)$$

where the angular brackets denote a time average. For independent time series,  $\gamma$  should be approximately zero, and close to unity if these are synchronized.

The onset of GS is indicated by an abrupt change in this order parameter; see Fig. 5 for the transition in case of the drive-response system. Subsequent to the transition,  $\gamma$  does not reach unity, implying that the degree of correlation (or synchrony) is nontrivial but not high due to the presence of noise. A similar transition occurs for the response and the auxiliary unit as shown in Fig. 5.

The order parameter  $\gamma$  shows a transition that is gradual and monotonic as a function of  $\varepsilon$ . In Fig. 5, which corresponds to the oscillatory state of the oscillator, the order parameter captures the transition at certain value of the coupling strength. Since the  $\gamma$  values are well below unity, implying a regime of weak generalized synchrony. The kink at  $\varepsilon = 0.2$  again is indicative of phase synchrony between the two units.

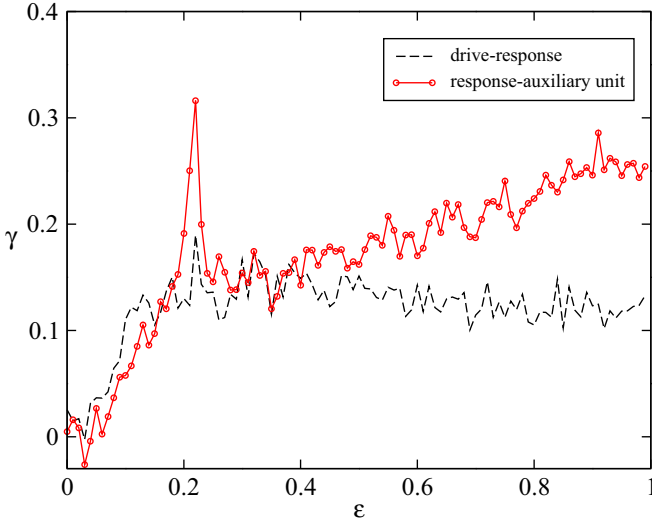


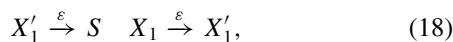
FIG. 5. Order parameter  $\gamma$  calculated by using the permutation entropy for the system given by Eqs. (6), (8), and (10) when the dynamics is oscillatory for the parameter values  $c_1 = 2.25 \times 10^4$ ,  $c_2 = 50$ ,  $c_3 = 5 \times 10^{-5}$ ,  $c_4 = 25$ ,  $V = 0.1$ ,  $\sigma = 10$ ,  $b = 8/3$ ,  $r = 28$  between drive and response, i.e.,  $\gamma_{x'x'}$  (dashed line) and the response and the auxiliary units  $\gamma_{x'x''}$  (red circle).

### III. APPLICATION: COUPLED CHEMICAL OSCILLATORS

We consider a situation where the response and drive are both chemical oscillators, namely when  $\mathbf{X}_i, i = 1, 2$  are stochastic signals. In a number of natural settings, the noise cannot be removed and therefore the coupling of intrinsically noisy dynamical systems [19] is of particular interest. Earlier studies have studied the synchronization of chaotic systems driven by “common” white noise [24,25], namely when the systems themselves are uncoupled but are influenced by the same background noise. GS in a noise-driven chaotic system with a linear synchronization function has been theoretically studied by constructing a response function using Lyapunov stability theory [31] and this technique was used to explore the existence of GS in chaotic systems on complex networks [32].

Since we are dealing with stochastic systems, the usual auxiliary system approach cannot be applied exactly, because the response and its auxiliary unit cannot be identical. We implement various techniques to detect GS in such a situation; these include correlation coefficients and the Mutual Information. Quantitative characterization of the dynamics is made via methods used in the study of complete synchronization in stochastic systems [29,33–35].

The coupled system can be written in terms of the “chemical” reactions described in Eqs. (A1) and (A2) (Appendix) together with



where species of the response will now be denoted by primed variables. Coupled auxiliary units can be produced

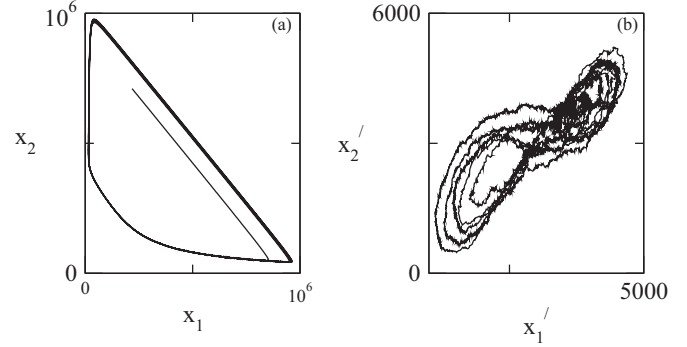
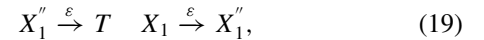


FIG. 6. Autonomous dynamics of (a) the drive, i.e., Brusselator Eqs. (A1), and the auxiliary unit at the parameter set  $c_1 = 5$ ,  $c_2 = 0.025$ ,  $c_3 = 5 \times 10^{-5}$ ,  $c_4 = 5$  and (b) the response, i.e., Lorenz Eqs. (A2), and the auxiliary unit for the parameter set  $c'_1 = 900$ ,  $c'_2 = 10$ ,  $c'_3 = 28$ ,  $c'_4 = 30$ ,  $c'_5 = 1$ ,  $c'_6 = 1$ ,  $c'_7 = 810$ ,  $c'_8 = 30$ ,  $c'_9 = 30$ ,  $c'_{10} = 10$ ,  $c'_{11} = 1$ ,  $c'_{12} = \frac{8}{3}$  at  $V = 100$ .

by appending the following reactions in Eq. (A2),



where the species of the auxiliary unit will be denoted by  $X''_1$ ,  $X''_2$ , and  $X''_3$ .

In the thermodynamic limit, the corresponding mass-action (deterministic) reaction rate equations are given by Eqs. (6) and (8) in the limit  $V \rightarrow \infty$ .

Carrying out the simulations using the stochastic simulation algorithm (SSA) [36], the attractors for the uncoupled chemical oscillators is described in Fig. 6(a) for the Brusselator and Fig. 6(b) for the Lorenz system depicting two entirely different dynamical systems that are intrinsically stochastic and are coupled through a drive-response relationship. We consider the set of parameter values where the dynamical behavior of the two systems is oscillatory. Figure 8 shows different regimes.

We now calculate the correlation between the two variables, i.e.,  $x-x'$  (drive-response) and  $x'-x''$  (auxiliary units) using Eq. (11).

As shown in Fig. 7, the correlations grow with increase in coupling. As the coupling increases, we observe that there is an increase in the correlation of the two systems ( $\rho_{xx'}$ ). The coupling value after which the correlations remain constant indicates the regime of GS. This observation is further strengthened by the fact that the correlation between the response and the auxiliary unit,  $\rho_{x'x''}$ , becomes close to unity at the same coupling values. Since the intrinsic time scales of oscillation of the two types of oscillators differs (although not drastically so), the response and the auxiliary being the same type of system become more correlated, while a lower level of correlation is achieved between the drive-response. The time series, shown in Fig. 8 for the drive-response and auxiliary unit, shows this quite dramatically. When there is no coupling [Fig. 8(a)] or it is very small [Fig. 8(b)], the time series of the units are completely uncorrelated, while the correlation between them increases as we increase the coupling [Fig. 8(c)] and, finally, the units are in synchrony for strong coupling [Fig. 8(d)] and subsequently remain in GS.

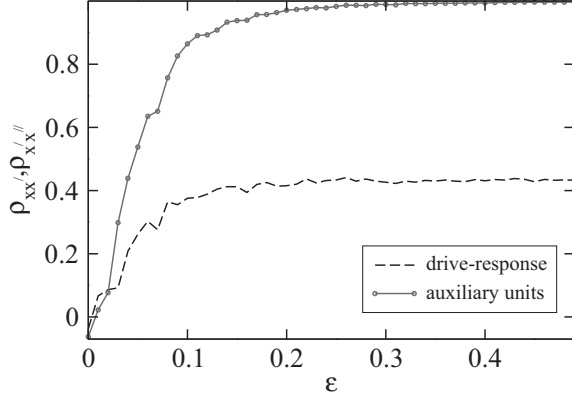


FIG. 7. Correlation for the system given by Eqs. (A1) and (A2), and the auxiliary unit for the parameter values  $c_1 = 5$ ,  $c_2 = 0.025$ ,  $c_3 = 5 \times 10^{-5}$ ,  $c_4 = 5$ ,  $c'_1 = 900$ ,  $c'_2 = 10$ ,  $c'_3 = 28$ ,  $c'_4 = 30$ ,  $c'_5 = 1$ ,  $c'_6 = 1$ ,  $c'_7 = 810$ ,  $c'_8 = 30$ ,  $c'_9 = 30$ ,  $c'_{10} = 10$ ,  $c'_{11} = 1$ ,  $c'_{12} = \frac{8}{3}$ ,  $c''_1 = 900$ ,  $c''_2 = 10$ ,  $c''_3 = 28$ ,  $c''_4 = 30$ ,  $c''_5 = 1$ ,  $c''_6 = 1$ ,  $c''_7 = 810$ ,  $c''_8 = 30$ ,  $c''_9 = 30$ ,  $c''_{10} = 10$ ,  $c''_{11} = 1$ ,  $c''_{12} = \frac{8}{3}$  at  $V=100$  between drive and response, i.e.,  $\rho_{XX'}$  (dashed line) and between the response and the auxiliary unit, i.e.,  $\rho_{X'X''}$  (red circle).

### A. Information-theoretic measures

In this section we again employ the information-theoretic measure, the Mutual Information [Eq. (13)], to study synchronization between the coupled units.

As shown in Fig. 9, the MI first increases with the increase in coupling. At lower coupling values the MI between the

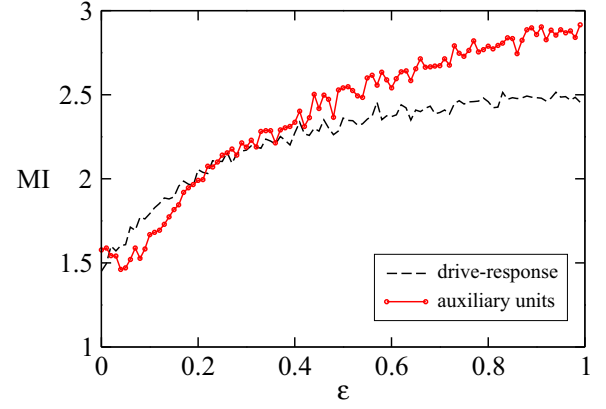


FIG. 9. Mutual information for the system given by Eqs. (A1) and (A2), and the auxiliary unit, for the parameter values  $c_1 = 5$ ,  $c_2 = 0.025$ ,  $c_3 = 5 \times 10^{-5}$ ,  $c_4 = 5$ ,  $c'_1 = 900$ ,  $c'_2 = 10$ ,  $c'_3 = 28$ ,  $c'_4 = 30$ ,  $c'_5 = 1$ ,  $c'_6 = 1$ ,  $c'_7 = 810$ ,  $c'_8 = 30$ ,  $c'_9 = 30$ ,  $c'_{10} = 10$ ,  $c'_{11} = 1$ ,  $c'_{12} = \frac{8}{3}$ ,  $c''_1 = 900$ ,  $c''_2 = 10$ ,  $c''_3 = 28$ ,  $c''_4 = 30$ ,  $c''_5 = 1$ ,  $c''_6 = 1$ ,  $c''_7 = 810$ ,  $c''_8 = 30$ ,  $c''_9 = 30$ ,  $c''_{10} = 10$ ,  $c''_{11} = 1$ ,  $c''_{12} = \frac{8}{3}$  between drive and response (dashed line) and between the response and the auxiliary unit (red circle).

drive-response (black) and response-auxiliary unit (red) is low, which increases and, finally, becomes constant as one increases the coupling between the two systems. The higher values of MI at larger coupling values clearly captures the onset of generalized synchrony in the system.

## IV. SUMMARY AND DISCUSSION

In the present work we have shown that stochastic systems can also show an analog of generalized synchrony by becoming strongly correlated with one another. We have mainly considered noisy systems coupled in a drive-response configuration. Application is made to model systems such as the Lorenz system being driven by a Brusselator, both simulated within the Langevin formalism [15]. For completeness, we have also studied Brusselator and Lorenz systems as coupled chemical oscillators, the coupling being in a drive-response relationship and examined the different regimes, ranging from the desynchronized state for low coupling to phase synchronization at higher coupling and eventually to GS.

In order to detect the synchronization behavior of noisy systems, though, it is necessary to examine measures based on the correlation between the variables of the drive and the response. Order parameters that are derived from the mutual information and the permutation entropy of a symbolic coding of the signals provide suitable measures to detect the transition from unsynchronized motion to generalized synchrony.

Generalized synchrony expands the notion of synchrony to the situation when systems become specifically correlated without necessarily behaving identically. Stochastic generalized synchrony can thus provide a framework within which the emergence of correlations in noisy systems can be understood. In one scenario, a signal from one dynamical system drives another [8] and causes the response to be functionally dependent on the drive. Noise-induced

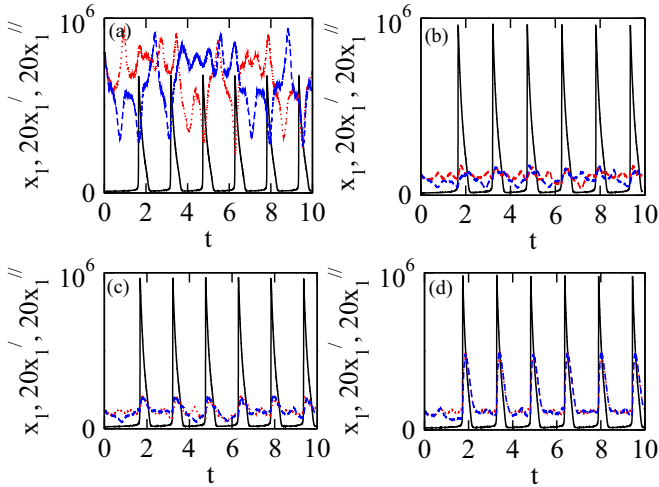


FIG. 8. Time series at different coupling values for the parameter set  $c_1 = 5$ ,  $c_2 = 0.025$ ,  $c_3 = 5 \times 10^{-5}$ ,  $c_4 = 5$ ,  $c'_1 = 900$ ,  $c'_2 = 10$ ,  $c'_3 = 28$ ,  $c'_4 = 30$ ,  $c'_5 = 1$ ,  $c'_6 = 1$ ,  $c'_7 = 810$ ,  $c'_8 = 30$ ,  $c'_9 = 30$ ,  $c'_{10} = 10$ ,  $c'_{11} = 1$ ,  $c'_{12} = \frac{8}{3}$ ,  $c''_1 = 900$ ,  $c''_2 = 10$ ,  $c''_3 = 28$ ,  $c''_4 = 30$ ,  $c''_5 = 1$ ,  $c''_6 = 1$ ,  $c''_7 = 810$ ,  $c''_8 = 30$ ,  $c''_9 = 30$ ,  $c''_{10} = 10$ ,  $c''_{11} = 1$ ,  $c''_{12} = \frac{8}{3}$  at  $V = 100$  for (a)  $\varepsilon = 0$ , (b)  $\varepsilon = 0.05$ , (c)  $\varepsilon = 0.1$ , and (d)  $\varepsilon = 0.4$ . The time series shown here represent the increase in the degree of synchronization with increase in coupling parameter. As the coupling increases, the drive (solid black line), response (dotted red line), and the auxiliary unit (dashed blue line) are synchronized, indicating the onset of generalized synchrony.

synchronization can be seen as an example of this phenomenon, with the external signal being a stochastic noisy drive [37,38]. Indeed GS has been shown to be noise resistant [39], and within a regime of GS the effect of noise is to confer greater stability to the system [17]. A related noise-induced coherence is the so-called *stochastic resonance* [40,41] and that phenomenon is of interest in its own accord.

Synchronization is arguably the most commonly observed collective behavior in a variety of natural systems [4]. Noise—both intrinsic and extrinsic—is also characteristic of such systems, and thus the persistence of synchrony in the presence of noise indicates that the phenomenon is robust [42]. Several instances of systems that individually are stochastic, but can nevertheless behave synchronously, have been reported, ranging from the case of coupled weather systems to coupled neurons or chemical oscillators to the so-called Moran effect [43], namely the synchronization of animal populations over wide areas due to correlations in environmental fluctuations (as, for example, in the weather) [44]. An example that underscores the importance of synchrony in the presence of intrinsic noise is in cellular dynamics: Microarray experiments of yeast have revealed that the dynamical behavior of sets of very distinct genes can be very similar [20,45]. The ubiquity of stochasticity in natural systems can thus give rise to a form of dependent dynamics that can provide a very robust mechanism for timekeeping.

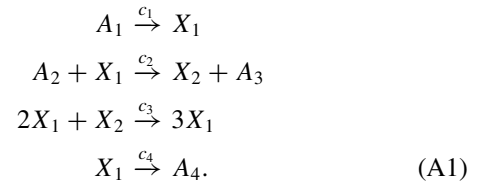
**ACKNOWLEDGMENTS**

H.H.J. thanks the UGC, India, for Grant No. F:30-90/2015 (BSR). R.K.B.S. acknowledges the Department of Science and Technology (DST), New Delhi, India, under sanction no. SB/S2/HEP-034/2012. R.R. acknowledges the Department of Science and Technology for support through the J. C. Bose National Fellowship.

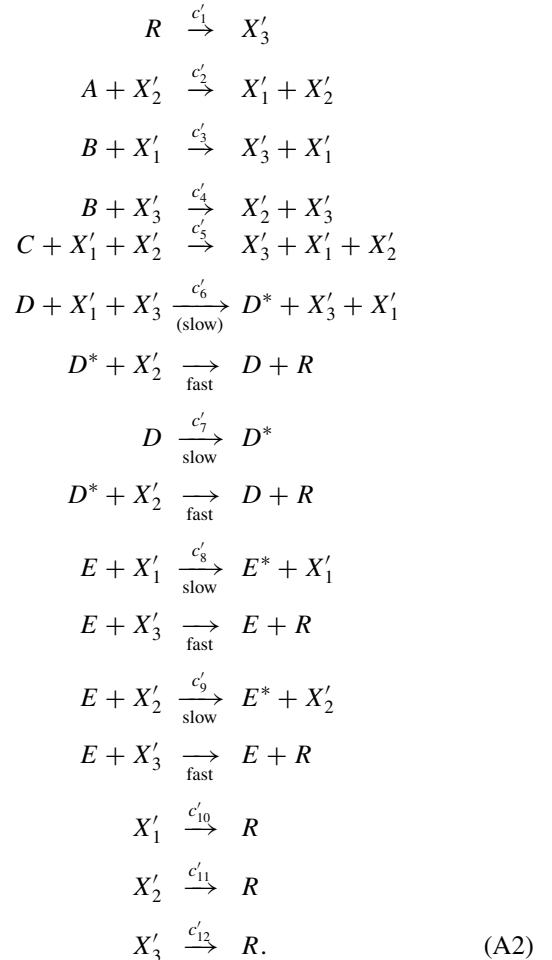
**APPENDIX: MODEL CHEMICAL OSCILLATORS**

Model coupled stochastic systems such as the Brusselator [36] and the Lorenz [22] are used in this study. The Brusselator model can be expressed in terms of the following

chemical equations:



The reaction mechanism for the Lorenz system is given by [22]



Both drive and response systems are treated using the exact (SSA) [36].

---

[1] A. Pikovsky, M. Rosenblum, and J. Kurths, *Synchronisation: A Universal Concept in Nonlinear Science* (Cambridge University Press, Cambridge, 2001).

[2] Q. Y. Wang, Q. S. Lu, G. R. Chen, and D. H. Guo, *Phys. Lett. A* **356**, 17 (2006).

[3] J. W. Shuai and D. M. Durand, *Phys. Lett. A* **264**, 289 (1999).

[4] L. Glass, *Nature (London)* **410**, 277 (2001).

[5] R. Roy, *Nature (London)* **438**, 298 (2005).

[6] H. Jaeger and H. Haas, *Science* **304**, 78 (2004).

[7] S. L. Scott, *ACM SIGOPS Op. Sys. Rev.* **30**, 26 (1996).

[8] N. F. Rulkov, M. M. Sushchik, and L. S. Tsimring, *Phys. Rev. E* **51**, 980 (1995).

[9] B. R. Hunt, E. Ott, and J. A. Yorke, *Phys. Rev. E* **55**, 4029 (1997).

[10] K. Pyragas, *Phys. Rev. E* **54**, R4508 (1996).

[11] M. G. Vilar, H. Y. Kueh, N. Barkai, and S. Leibler, *Proc. Natl. Acad. Sci. USA* **99**, 5988 (2002).

[12] Y. Y. Goldschmidt, H. Hinrichsen, M. Howard, and U. C. Täuber, *Phys. Rev. E* **59**, 6381 (1999).

[13] G. C. Graham and O. Lipan, *J. Biol. Phys.* **37**, 441 (2011).

[14] J. H. Abel, L. A. Widmer, P. C. S. John, J. Stelling, and F. J. Doyle, *IEEE Life Sci. Lett.* **1**, 3 (2015).

[15] D. T. Gillespie, *J. Chem. Phys.* **113**, 297 (2000).

[16] S. Guan, Y. C. Lai, and C. H. Lai, *Phys. Rev. E* **73**, 046210 (2006).

- [17] O. I. Moskalenko, A. E. Hramov, A. A. Koronovskii, and A. A. Ovchinnikov, *Eur. Phys. J. B* **82**, 69 (2011).
- [18] P. Érdi and J. Tóth, *Mathematical Models of Chemical Reactions: Theory and Applications of Deterministic and Stochastic Models* (Manchester University Press, Manchester, UK, 1989).
- [19] N. G. van Kampen, *Stochastic Processes in Physics and Chemistry* (Elsevier, Amsterdam, 2007).
- [20] The high level of interrelatedness among biochemical pathways in a cell underlies the complexity of metabolic and genomic networks. For a striking example, see B. P. Tu, A. Kudlicki, M. Rowicka, and S. L. McKnight, *Science* **310**, 1152 (2005).
- [21] I. Prigogine and R. Lefever, *J. Chem. Phys.* **48**, 1695 (1968); J. J. Tyson, *ibid.* **58**, 3919 (1973).
- [22] D. Poland, *Physica D* **65**, 86 (1993).
- [23] L. Kokarev and U. Parlitz, *Phys. Rev. Lett.* **76**, 1816 (1997).
- [24] A. Maritan and J. R. Banavar, *Phys. Rev. Lett.* **72**, 1451 (1994).
- [25] R. Toral, C. R. Mirasso, E. H. Garcia, and O. Piro, *Chaos* **11**, 665 (2001).
- [26] We employ the Euler-Maruyama method that is derived from the Itô scheme [19] as discussed in, for example, D. J. Higham, *SIAM Rev.* **43**, 525 (2001).
- [27] T. M. Cover and J. A. Thomas, *Elements of Information Theory* (Wiley, New York, 1991).
- [28] C. E. Shannon and W. Weaver, *The Mathematical Theory of Information* (University of Illinois Press, Urbana, 1989).
- [29] C. Brandt and B. Pompe, *Phys. Rev. Lett.* **88**, 174102 (2002).
- [30] Z. Liu, *Europhys. Lett.* **68**, 19 (2004).
- [31] A. Hu and Z. Xu, *Phys. Lett. A* **372**, 3814 (2008).
- [32] A. Hu, Z. Xu, and L. Guo, *Chaos* **20**, 013112 (2010).
- [33] J. S. Canovas and A. Guillamon, *Chaos* **19**, 043103 (2009).
- [34] R. Monetti, W. Bunk, and T. Aschenbrenner, and F. Jamitzky, *Phys. Rev. E* **79**, 046207 (2009).
- [35] Y. Cao, W. Tung, J. B. Gao, V. A. Protopopescu, and L. M. Hively, *Phys. Rev. E* **70**, 046217 (2004).
- [36] D. T. Gillespie, *J. Phys. Chem.* **81**, 2340 (1977).
- [37] S. Fahy and D. R. Hamann, *Phys. Rev. Lett.* **69**, 761 (1992).
- [38] A. E. Hramov, A. A. Koronovskii, and O. I. Moskalenko, *Phys. Lett. A* **354**, 423 (2006).
- [39] A. A. Koronovskii, O. I. Moskalenko, A. A. Ovchinnikov, and A. E. Hramov, *Bull. Russ. Acad. Sc. Phys.* **73**, 1616 (2009).
- [40] R. Benzi, A. Sutera, and A. Vulpiani, *J. Phys. A* **14**, L453 (1981).
- [41] A. Longtin and D. R. Chialvo, *Phys. Rev. Lett.* **81**, 4012 (1998).
- [42] A. Nandi, G. Santosh, R. K. B. Singh, and R. Ramaswamy, *Phys. Rev. E* **76**, 041136 (2007); A. Nandi and B. Lindner, *Chem. Phys.* **375**, 348 (2010).
- [43] P. A. P. Moran, *Aust. J. Zool* **1**, 291 (1953).
- [44] T. M. Massie, G. Weithoff, N. Kuckländer, U. Gaedke, and B. Blasius, *Nat. Commun.* **6**, 5993 (2015).
- [45] S. Tavazoie, J. D. Hughes, M. J. Campbell, R. J. Cho, and G. M. Church, *Nat. Genet.* **22**, 281 (1999).